CrossMark

ORIGINAL ARTICLE

The combined effect of Persian Gulf and Mediterranean Sea surface temperature on operational forecast of spring streamflow for Karkheh basin, Iran

Fereshteh Modaresi[1] · Shahab Araghinejad[1] · Kumars Ebrahimi[1]

Abstract In this study, it has been investigated whether the SSTs of *Mediterranean Sea* and *Persian Gulf* and combination of them are applicable and effective variables as predictors for operational streamflow forecasting, regionally, in *Karkheh* basin or not. For this goal, the singular value decomposition (SVD) method has been used to determine the effective nodes of *Mediterranean Sea* and *Persian Gulf* on the climate of the subbasins of this basin and to produce the most correlated time series of SST with the streamflow of each subbasin. In this research, the best predictors have been detected from several combinations of the appropriate predictors based on the cross-validation analysis for the results of the Generalized Regression Neural-Network model. Results show that autumn SST of *Mediterranean Sea* and *Persian Gulf* is prominently effective variables for forecasting the streamflow in all subbasins of *Karkheh* basin in April and May, respectively. Summer SST of *Persian Gulf* has been detected as an effective predictor for streamflow forecasting in April and May in snowy regions. Moreover, the results demonstrate that the combination of *Mediterranean Sea* SST and *Persian Gulf* SST affects the streamflow in almost all the regions of the basin in April, while the streamflow in May is affected only by *Persian Gulf* SST. In addition, the north and west regions of *Karkheh* basin (*Garsha* and *Seimareh* subbasins) as well as the east and south regions of this basin (*Tang Mashooreh* and *Karkheh* subbasins) have similar pattern of the best predictors for operational streamflow forecasting in all the spring months.

Introduction

Karkheh basin is one of the large basins in the west of Iran which is a part of *Persian Gulf* basin. This basin with an area of 50,764 km^2 lies between latitudes 33°40′ and 35°00′N, and longitudes 46°23′ and 49°12′E, where *Hamedan*, *Kermanshah*, *Ilam*, *Lorestan*, and *Khoozestan* provinces are located. Figure 1 shows the location of *Karkheh* basin in the provinces. Because of its large area, *Karkheh* basin has a variety of weather conditions, such that its southern areas are semiarid with mild winters and long and warm summers, while the northern regions of this basin, which are mountainous areas, have cold winters and mild summers. The temperature in this basin varies from −25 to 50 °C. The average of annual precipitation is ranged from 300 to 800 mm. Overall, *Karkheh* basin has *Mediterranean* climate. The major sources of precipitation in the study basin are moist air flows which get to the area along with low-pressure centers that originate from *Mediterranean Sea*, *Persian Gulf*, and *Black Sea*. The annual frequency of the low-pressure centers of *Mediterranean Sea*, *Persian Gulf*, and *Black Sea* is 64.5, 22.9, and 6.12 %, respectively.

The main river of the basin is *Karkheh* River formed at the beginning of two branches: *Gamasiab* in the northeast

✉ Fereshteh Modaresi
fmodaresi@ut.ac.ir

Shahab Araghinejad
araghinejad@ut.ac.ir

Kumars Ebrahimi
EbrahimiK@ut.ac.ir

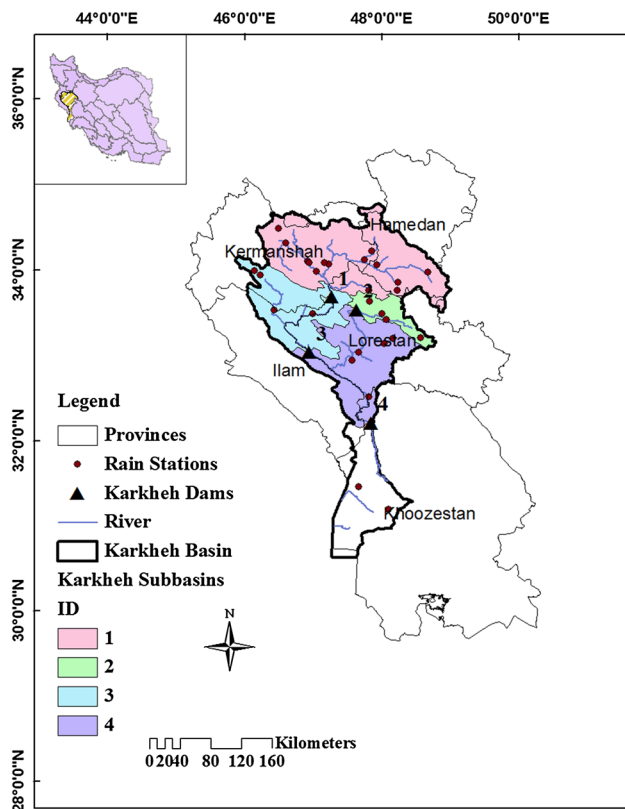[1] University of Tehran, Tehran, Iran

Fig. 1 Location of Karkheh basin and its subbasins, rivers, reservoirs, and rain stations

and *Gharesu* in the northwest. The two rivers join together at the end of *Kermanshah* plain and make up *Seimareh River*. The confluence of *Seimareh* and *Kashkan* River, which originates from the east part of the basin, forms *Karkheh River*. The rivers of *Karkheh* basin supply domestic, agricultural, and industrial water demands of the five provinces. Therefore, long-lead streamflow forecasting of the each river plays an important role in water resources management for this basin and its provinces.

In a variety of the researches, ocean-atmospheric variables, such as El Niño-Southern Oscillation (ENSO), Pacific Decadal Oscillation (PDO), the Southern Oscillation Index (SOI), the North Atlantic Oscillation (NAO), and Atlantic Multi decadal Oscillation (AMO), have been applied as predictors for long-lead hydrological forecasting in all over the world (Hamlet and Lettenmaier 1999; Araghinejad et al. 2006; Karla and Ahmad 2009; Soukup et al. 2009; Dezfuli et al. 2010; Azimi et al. 2011; Lorenzo-lacruz et al. 2011; Tabari et al. 2013).

Sea surface temperature of oceans and seas is another variable, whose effectiveness on the meteorological and hydrological conditions of various areas all over the world has been proved in several studies (Nicholls 1989; Uvo et al. 1998; Wang and Ting 2000; Rodriguez-Fonseca and de Castro 2002; Tootle and Piechota 2006; Oubeidillah

et al. 2012; Sagarika et al. 2015); therefore, it has been applied as predictor for long-lead forecasting of rainfall and streamflow (Wallace et al. 1992; Nazemosadat 1998; Clark et al. 2000; Rowell 2003; Kassomenos and McGregor 2006; Tootle et al. 2007, 2008; Nazemosadat 2008; Lima and Lall 2010; Gamiz-Fortis et al. 2010; Oubeidillah et al. 2011; Meidani and Araghinejad 2014).

Mediterranean Sea is an important source of humidity in the west of Iran which affects the climate of its surrounding countries. For instance, the variability of sea-level pressure (SLP) of *Mediterranean Sea* in a region from Balkkans toward Arabian Peninsula in winter affects on rainfall in Turkey (Kutiel et al. 2001). In addition, the anomalies of *Mediterranean Sea* SST have positive correlation with total rainfall of the wet seasons over the Sahel in Africa (Rowell 2003). Moreover, the surface temperature, humidity, and atmospheric pressure data of *Mediterranean Sea* have an effect on estimating the variation of perceptible water content over southern Greece (Kassomenos and McGregor 2006). Besides, the autumn SST of *Mediterranean Sea* has an effect on winter precipitation and streamflow in southwest of Iran and it is considered as a predictor for winter streamflow forecasting (Meidani and Araghinejad 2014).

As *Mediterranean Sea* has large size and limited exchange at Gibraltar Strait, its dynamics is mainly linked to the local climate, and is particularly sensitive to anthropogenic climatic perturbations (Skiliris et al. 2011). In the winter of the northern hemisphere when the *Red Sea* and *Persian Gulf* act as powerful sources of water vapor, and cause little precipitation locally due to descending air in the Hadley cell, the *Mediterranean Sea* of low pressure lying between the two regions of high pressure in the North Atlantic, centered at about 30° N and those over Asia at about 45° N leads to the westerly prevailing winds along the north coast of Africa toward Iran (Kendrew 1922).

Another sea which affects on the climate of Iran is *Persian Gulf*. Nazemosadat (1998) proved that there is a significant negative correlation between SST of *Persian Gulf* and precipitation in winter in the provinces located in the west and south of Iran; such that when SST of *Persian Gulf* is less than the average, rainfall will be more than normal in this region. Based on this study, Nazemosadat (2008) used SST of *Persian Gulf* in autumn and winter to forecast precipitation in these seasons in Shiraz and Bushehr stations in southwestern Iran.

The best known phenomenon in the *Persian Gulf* which can cause abrupt changes in the circulation and heat budget for a short period of time is *shamal*, a northwesterly wind occurring during winter and summer (Perrone 1979). On the basis of duration, winter *shamal* includes two types of winds: those which last 24–36 h and those which last 3–5 days. The winds bring cold dry air ($T = 20$ °C) and result in cooling of SST about 10 °C noticeably in the

northern and shallower shelf regions (Thoppil and Hogan 2010). The other air masses which mostly affecting the area in winter is Sudan current. About 30 % of the total rain-bearing air masses coming to Iran originate in North Africa, Red Sea, and Saudi Arabia which is called Sudan current (Khalili 1992).

As the major sources of precipitation in the study basin are moist air flows which reach the area along with low-pressure centers that originate from *Mediterranean Sea, Persian Gulf,* and *Black Sea* with the annual frequency of 64.5, 22.9, and 6.12 %, respectively, the fluctuations of Sea Surface Temperature (SST) of *Mediterranean Sea* and *Persian Gulf* can affect on meteorological and hydrological conditions of this basin; therefore, they can be considered as effective predictors for meteorological and hydrological forecasting of the study basin.

Due to the fact that sea surface temperature (SST) variable is measured in a large number of grid cells, applying methods, such as Principal Component Analysis (PCA), or Singular Value Decomposition (SVD) is necessary to produce time series of SST having the highest correlation with predicted hydrological variables. In most of the studies in this field, the SVD method has been preferred and used (Wallace et al. 1992; Uvo et al. 1998; Rowell 2003; Soukup et al. 2009; Meidani and Araghinejad 2014), because the SVD method is able to evaluate two spatio-temporal variables, such as SST and precipitation or streamflow, in several stations using the cross-covariance matrix, while the PCA method only can evaluate one spatio-temporal variable.

In order to forecast hydrological variables in long-lead time intervals, ANN method has usually been used (Anctil and Rat 2005; Wang et al. 2009; Wu et al. 2010; Sattari et al. 2012; Meng et al. 2015). However, a number of researches have evaluated the performance of neural-network types, including Artificial Neural Network (ANN) with the structure of feed forward back propagation (FFBP), Generalized Regression Neural Network (GRNN), and Radial Basis Function (RBF) for monthly hydrological forecasting (Cigizoglu and Alp 2004; Cigizoglu 2005; Kisi 2008; Hosseini-Moghari and Araghinejad 2015). Their results unanimously indicates that the performance of GRNN model is better than other methods for hydrological forecasting in monthly time scale, because GRNN has not been faced the local minima problem, while FFBP has often encountered it. Besides, only GRNN technique has produced the results that all are physically possible, and they are not negative. Cigizoglu (2005) also compared the performance of GRNN with AR method, and the results indicated the superiority of GRNN for monthly forecasting.

In the light of what was said, as the major sources of precipitation in the *Karkheh* basin are the moist air flows that originate from *Mediterranean Sea, Persian Gulf,* and

Black Sea with the annual frequency of 64.5, 22.9, and 6.12 %, respectively, and in the previous researches, the effectiveness of *Mediterranean Sea* and *Persian Gulf* SST on the autumn and winter precipitation forecasting in a spread region in the west of Iran has been proved separately (Nazemosadat 1998; Nazemosadat 2008; Meidani and Araghinejad 2014), and due to the effect of winter precipitation on spring streamflow, the focus of this research is on investigation of the combined effect of *Mediterranean Sea* and *Persian Gulf* SST on operational streamflow forecasting in the west of Iran in spring. Indeed, we want to survey whether SSTs of both *Mediterranean Sea* and *Persian Gulf* are applicable and effective variables as predictors for operational streamflow forecasting, regionally, or not. Besides, we want to study the direct effect of *Mediterranean Sea* and *Persian Gulf* SST on streamflow forecasting without forecasting of precipitation to reduce the error of rainfall-runoff modeling from the final results. For this purpose, naturalized streamflow data affected directly by precipitation have been used. In addition, the SVD technique has been used in this study to recognize the effective nodes of *Mediterranean Sea* and *Persian Gulf* on the climate of the *Karkheh* basin and to produce the most correlated time series of SST with the streamflow of the basin. Because monthly time scale has been selected for streamflow forecasting, GRNN method has been preferred, based on the literature review, to apply for this study.

Data

Sea surface temperature (SST) of *Mediterranean Sea* and *Persian Gulf*

Sea surface temperatures of *Mediterranean Sea* and *Persian Gulf* are measured for 1° grid squares of the seas. Therefore, the overall surface of them is covered by 101 and 26 grid cells (node), respectively. Monthly average of SST for each grid cell (NOAA_OI_SST_V2) is available from November 1981 to present in the website (http://www.esrl.noaa.gov/psd). In this study, the seasonal average of SST in all grid cells from 1982 to 2007 has been used.

Hydrological and meteorological data

In this paper, the forecasting of spring monthly inflow to four reservoirs in *Karkheh* basin, including *Garsha, Tang Mashooreh, Seimareh,* and *Karkheh,* has been investigated. The position, ID (identification code), and the subbasin at the upstream of each reservoir have been illustrated in Fig. 1. It is noted that the ID of each reservoir is the same as its subbasin. As can be seen from Fig. 1, the reservoirs

390

Sustain. Water Resour. Manag. (2016) 2:387–403

collect the flows of all rivers overall the *Karkheh* basin. Table 1 shows the ID, name, location, and rivers of the dams. It is worth nothing that to describe the properties of each dam and related subbasin shown in Fig. 1 in Table 1, ID has been used jointly in Fig. 1 and Table 1.

Garsha and *Tangmashooreh* reservoirs collect the streamflow of the branches which have natural streams. However, *Seimareh* and *Karkheh* dams are located downstream of two other dams and the inflow to them is regulated. As climate indices affect the natural phenomena, the naturalized inflow data to these two reservoirs have been used in this research. To achieve the natural streamflow, which is affected directly by precipitation, and indeed, is the streamflow before every harvesting and use, the value of water harvesting from each section of the river has been added to the observed streamflow in the same section. It is noted that *Garsha* and *Tang Mashooreh* dams are in the study phase, while *Seimareh* and *Karkheh* dams are being exploited.

In addition to *Mediterranean Sea* and *Persian Gulf* SST, the monthly precipitation data of rain stations located in the upstream of dams have been utilized as predictors for forecasting the inflow to each reservoir. The distribution of rain stations in the subbasin of each dam and the number of them have been displayed in Fig. 1 and Table 1, respectively. The monthly hydrometrical and meteorological data have been available from 1957 to 2007; but because the SST data are available since November 1981, the hydrometrical and meteorological data in the period from 1982 to 2007 have been used in this paper.

Methodology

The current research has been done in three steps as follows:

Step 1   Applying SVD method to recognize the effective nodes of *Mediterranean Sea* and *Persian Gulf* on the climate of the *Karkheh* basin, and to produce the time series of SST and also precipitation of rain stations, such that they have the most correlation with the inflow to each of the reservoirs using the SVD technique

Step 2   Selecting the appropriate predictors for each month and each reservoir according to two evaluation criteria, including: correlation coefficient (R^2) and an index based on mutual information (MI) and entropy rules, MMI

Step 3   Forecasting of spring monthly inflow to each reservoir using GRNN method based on various combinations of predictors, and selecting the best final predictors for each reservoir and each month based on three assessment criteria, including: Nash–Sutcliff, root mean square error (RMSE), and correlation coefficient

In the following, the methods used for each step have been described.

Singular value decomposition (SVD)

SVD is a powerful statistical technique on the basis of a theorem from linear algebra. It is a data-mining procedure which can produce the most correlated series from a huge number of data. According to the SVD method, a rectangular matrix $\mathbf{A_{mn}}$ can be broken into the three matrices, including: an orthogonal matrix $\mathbf{U_{mm}}$, a diagonal matrix $\mathbf{S_{mn}}$, and the transpose of an orthogonal matrix $\mathbf{V_{nn}}$. Mathematically, it is represented as follows (Bretherton et al. 1992):

$$A_{mn} = U_{mm}S_{mn}V_{nn}^{T} \tag{1}$$

where $\mathbf{U^T U} = I_{mm}$, $\mathbf{V^T V} = I_{nn}$, and the columns of U are the left singular vectors, S has singular values, and V^T has rows which are the right singular vectors. The columns of $\mathbf{U}$ and $\mathbf{V}$ are made up of orthonormal eigenvectors of $\mathbf{AA^T}$ and $\mathbf{A^T A}$, respectively. Moreover, the singular values in $\mathbf{S}$ are square roots of eigenvalues from of $\mathbf{AA^T}$ or $\mathbf{A^T A}$ which are arranged in descending order.

The procedure of applying SVD to produce correlated series from predictor variables (such as SST of *Persian Gulf* in 26 points) and forecasted variables (inflow to the four reservoirs of *Karkheh* basin) for 25 years is presented here. First, the cross-covariance matrix of the standardized values of *Persian Gulf* SSTs and streamflow data should be produced as follows:

Table 1 Properties of Karkheh reservoirs

ID	Name	Location		Name of rivers	Number of rain stations
		Latitude	Longitude		
1	Garsha	47°28′58″	33°56′32″	Gamasiab and Ghare su	15
2	Tang Mashooreh	47°50′18″	33°48′32″	Kashkan	3
3	Seimareh	47°12′47″	33°16′41″	Seimareh	6
4	Karkheh	48°07′31″	32°29′22″	Karkheh	5

$$
\text{COVAR} = \frac{1}{y} \times \begin{bmatrix} sst_{1,1} & \cdots & sst_{1,y} \\ \vdots & \ddots & \vdots \\ sst_{g,1} & \cdots & sst_{g,y} \end{bmatrix}
$$
$$
\times \begin{bmatrix} q_{1,1} & \cdots & q_{1,s} \\ \vdots & \ddots & \vdots \\ q_{y,1} & \cdots & q_{y,s} \end{bmatrix} \tag{2}
$$

where g is the number of SST's grid cells, y is the number of years, and s represent the number of streamflow stations.

Then, applying the SVD method for the above matrix yields two orthogonal matrices (U_{gg} and V_{ss}) containing singular vectors and a diagonal matrix (S_{gs}) containing the singular values, among which the following relation is established:

$$
\text{SVD}(\text{COVAR}_{gs}) = U_{gg} S_{gs} V_{ss}^{T}. \tag{3}
$$

As previously mentioned, Matrix S is a diagonal matrix containing singular values arranged in descending order. To compare the relative importance of modes based on the singular values, the squared covariance fraction (SCF) as a useful measurement has been used (Bretherton et al. 1992). It is defined as follows:

$$
\text{SCF}_j = \frac{C_j^2}{\sum C^2} \tag{4}
$$

where C_j represents each of the singular values. When the SCF value of the first mode is too higher than the others, the temporal expansion series can be obtained by projecting the data onto the first column of singular vector matrices. For example, the projected temporal expansion series of SST (SSTP) and streamflow (QP) for the first mode is computed with $i = 1$ in Eq. 5:

$$
\text{SSTP}(i) = \begin{bmatrix} sst_{1,1} & \cdots & sst_{1,g} \\ \vdots & \ddots & \vdots \\ sst_{y,1} & \cdots & sst_{y,g} \end{bmatrix} U(:,i)
$$
$$
\text{QP}(i) = \begin{bmatrix} q_{1,1} & \cdots & q_{1,s} \\ \vdots & \ddots & \vdots \\ q_{y,1} & \cdots & q_{y,s} \end{bmatrix} V(:,i). \tag{5}
$$

In the above equation, i can vary from 1 up to the maximum number of significant modes.

In the present study, the SVD method has been applied for the streamflow in each of the spring months and the seasonal average SST of *Persian Gulf* and *Mediterranean Sea* in the last winter, autumn, and summer, in all grid points (101 grids in *Mediterranean Sea* and 26 grids in *Persian Gulf*). Using SVD, a projected series of SST, having the highest correlation with the streamflow, has been produced for each season.

Moreover, the SVD technique has been applied for monthly rainfall of the stations at the upstream of each reservoir and the monthly inflow to the reservoir. Consequently, using SVD, a projected series of rainfall has been achieved for each month which has a higher correlation with the inflow than the average of the rainfall of the stations. This process has been repeated for a time delay of 1–5 months.

Evaluation criteria for the selection of the appropriate predictors

To select the appropriate predictors, the correlation coefficient (CORR) has been used to discover the linear correlations between predictors and forecasted variables. Mutual Information Index (MI) also represents a general information theoretic approach to determine the statistical dependence between variables. MI has been developed in hydro-climatic issues by a presented approach that identifies optimal predictors for rainfall probabilistic forecasting (Sharma 2000). This index determines the mutual information between two data series x and y, and because of having density-based formulation, it is able to recognize nonlinear dependence patterns.

In this research, an index based on Mutual Information index (MI) and entropy roles, MMI, has been presented and applied to determine the nonlinear correlations. If x and y are the representative of predictor and forecasted variables, respectively, MMI is defined as follows:

$$
\text{MMI} = \frac{\text{MI}(x,y)}{\min(H(x), H(y))} \tag{6}
$$

where MI (x,y) is the Mutual Information index, and $H(x)$ and $H(y)$ are the 'simple' entropy of the time series x and y calculated as follows (Gray 2013):

$$
\text{MI}(x,y) = \sum_{y \in Y} \sum_{x \in X} p(x,y) \log\left(\frac{p(x,y)}{p(x)p(y)}\right) \tag{7}
$$

$$
H(x) = -\sum_{x \in X} p(x) \log p(x) \geq 0
$$
$$
H(y) = -\sum_{y \in Y} p(y) \log p(y) \geq 0 \tag{8}
$$

where $p(x,y)$ is the joint probability density function of x and y, and $p(x)$ and $p(y)$ are the marginal probability density functions of x and y, respectively. If x and y are independent, i.e., x does not give any information about y and vice versa, their MI will be zero. The strong dependence between two variables results in a high value of MI.

Based on entropy rules, the range of MI is as follows (Gray 2013):

$$0 \leq \mathrm{MI}\,(x, y) \leq \min(H(x), H(y)). \tag{9}$$

Therefore, the range of the MMI index is between 0 and 1, such that if data series x and y are independent completely, their MMI will be zero, and if they are dependent completely, their MI is equal to minimum of $H(x)$ and $H(y)$, and therefore, their MMI will be equal to one. While MI index has not a constant upper limit, the constant range of MMI allows the user to select simply the appropriate predictors based on a specified limit.

In the current study, to select the appropriate predictors for forecasting of inflow to each reservoir in each of the spring months, the monthly streamflow and precipitation (projected series of rainfall resulted from SVD method) with a time delay of 1–5 months, and a seasonal projected series of *Mediterranean Sea* and *Persian Gulf* SST have been evaluated according to these two evaluation criteria.

Forecasting procedure

Generalized regression neural network (GRNN)

The generalized regression neural network (GRNN) is a variant of the radial basis function (RBF) network. It is a universal approximator for smooth functions, and is able to solve any smooth function-approximation problem with enough data. The GRNN considers each of the experienced pairs of data as a possible class that is probably to happen with respect to the observation of specific conditions (Araghinejad 2014).

GRNN is a three layer network in which the number of neurons in the input and output layers, such as the most neural networks, is equal to the dimension of input and output vectors, respectively. However, unlike other networks, the number of neurons in the hidden layer of this network is equal to the number of observed data.

In this model, a Gaussian performance function is applied in each of the neurons in the hidden layer and the input data to this function for each neuron is the Euclidian distance between new input vector to the neuron and the vector of the same size of the input specified to that neuron. The Gaussian function is as follows (Araghinejad 2014):

$$\begin{aligned} f(X_r, b) &= e^{-I^2} \\ I &= \|X_r - X_b\| \times 0.8326/h \end{aligned} \tag{10}$$

where X_r is the network input vector with unknown output, X_b is the observed input vector in time or location b, and h is the *spread* parameter of the Gaussian function (a type of radial basis function). The output of the function is between 0 and 1, such that when $\|X_r - X_b\|$ approaches to zero, the output approaches to 1. In addition, when it approaches to a large value, the output approaches to 0.

The output of the GRNN is calculated by the following equation (Araghinejad 2014):

$$Y_r = \frac{1}{\sum_{b=1}^{n} f(X_r, b)} \sum_{b=1}^{n} [f(X_r, b) \times T_b] \tag{11}$$

where T_b is the target associated with the bth observation, and n is the number of observations.

Assessment criteria for the evaluation of forecasting

To evaluate the forecasting results, in addition to two well-known criteria, including root mean square error (RMSE) and correlation coefficient (CORR), the Nash–Sutcliff efficiency coefficient has been applied between observed and forecasted data. The Nash–Sutcliff index has been presented in 1970 by Nash and Sutcliff to evaluate the predictive power of hydrological models (Nash and Sutcliffe 1970). It is defined as follows:

$$E = 1 - \frac{\sum_{t=1}^{T} \left(Q_o^t - Q_m^t\right)^2}{\sum_{t=1}^{T} \left(Q_o^t - \bar{Q}_o\right)^2} \tag{12}$$

where $\bar{Q}_o$ is the mean of observed streamflow, and Q_m^t and Q_o^t are the estimated and observed streamflows at time t, respectively. The range of this index is from $-\infty$ to 1. The efficiency of 1 ($E = 1$) means that the modeled streamflow corresponds to the observed data, while $E = 0$ indicates that the model estimations are equal to the mean of observed data and $E < 0$ demonstrates that the residual variance, calculated in the numerator of Eq. (12), is larger than the data variance, calculated in the denominator of that. As a result, the closer values of model efficiency to 1 indicate the more accurate results of the model.

Result and discussion

As the study has been done in three steps, the results of each step have been presented separately as follows.

Results of SVD analysis

The first mode SCF resulted from the SVD analysis for all the nodes of *Mediterranean Sea* and *Persian Gulf* was above 95 % in all the cases. As a result, it can be concluded that the SST of all the nodes of these two seas affect on the study region. As the vast majority of the variability in the data is explained in the first mode, the projected series obtained from the first mode of SVD has been applied as probable predictors in this study.

Moreover, the first mode SCF resulted from the SVD analysis for the precipitation of rain stations and inflow to

the reservoirs was above 90 % in all the cases. Thus, the rainfall projected series obtained from the first mode of SVD has been used as probable predictors rather than the average precipitation of the rain stations in this study.

Results of selecting the appropriate predictors

Among all the considered variables as probable predictors, the variables which had the correlation coefficient (CORR) or the modified mutual information (MMI) greater than 0.5 with the forecasted variable have been chosen as the appropriate predictors for modeling in the present paper. The appropriate streamflow predictors for each reservoir and each month have been presented in Table 2.

As can be seen from Table 2, several variables have been detected as selected predictors for each reservoir and each month. However, it can be prominently recognized that summer, autumn, and winter projected a series of *Persian Gulf* SST have high correlation and/or mutual information with the inflow to all reservoirs in May and June. In addition, an autumn projected series of *Mediterranean Sea* SST has high correlation and mutual information with the inflow to all reservoirs in April. Moreover, a rainfall projected series in March and monthly streamflow in April and May have high correlation and/or mutual information with the inflow to all reservoirs in April, May, and June, respectively.

Results of forecasting

To calibrate the GRNN model in training phase, on the one hand, the optimum value of *Spread* parameter should be determined, such that the error of forecasting will be the lowest one. On the other hand, although a number of variables have been chosen as candidate streamflow predictors for each month and each reservoir based on CORR and MMI criteria, applying all of them together does not necessarily lead to the best results of forecasting. Therefore, various combinations of the candidate predictors have been tested using GRNN model, and for each of the combinations, the cross-validation analysis has been done to determine the best value of *Spread* parameter (from the range between 0.1 and 7 with the steps 0.1) which results in the lowest error for the considered combination of the predictors. The best obtained results of the model for each combination of the predictors (resulted from the best value of *Spread* parameter) have been evaluated according to three criteria, Nash–Sutcliff, RMSE, and CORR. Finally, according to the best results, the best combination of the predictors has been determined for each month and each dam.

Table 3 shows the best predictors and their assessment criteria resulted from the cross-validation analysis of 25 streamflow forecasts not used in the calibration phase for each reservoir for April. Tables 4 and 5 illustrate similar results for May and June, respectively.

It can be seen from Table 3 that the autumn projected series of *Mediterranean Sea* SST is an effective predictor for forecasting the inflow to all reservoirs in April. Summer projected series of *Persian Gulf* SST also affects the inflow to *Garsha* reservoir in April. To forecast the inflow to *Tang Mashooreh* and *Karkheh* reservoir in April, winter projected series of *Persian Gulf* SST is an effective predictor. Rainfall projected series in March is useful predictors for

Table 2 Selected predictors for forecasting the spring monthly inflow to each of the reservoirs

Predictors		Forecasted variable: monthly streamflow											
		Garsha			*Tang Mashooreh*			*Seimareh*			*Karkheh*		
Type	Description	April	May	June	April	May	June	April	May	June	April	May	June
Persian Gulf SST	Summer projected series	✔*	✔*	✔*	✔	✔*	✔*		✔*	✔*		✔*	✔*
	Autumn projected series		✔	✔		✔*	✔*		✔*	✔*		✔*	✔*
	Winter projected series		✔	✔*	✔*	✔*	✔*		✔		✔*	✔*	✔*
Mediterranean Sea SST	Autumn projected series	✔*			✔*			✔*	✔*	✔*	✔*		✔
Monthly rainfall	Rainfall projected series in March	✔*				✔		✔	✔*	✔*	✔*	✔*	✔
	Rainfall projected series in April		✔*										
	Rainfall projected series in May			✔*			✔*						✔*
Monthly streamflow	Streamflow in March	✔					✔						✔
	Streamflow in April		✔	✔	✔	✔		✔				✔	✔*
	Streamflow in May			✔*			✔*			✔*			✔*

✔*: Both MMI and CORR are greater than 0.5; ✔: Either MMI or CORR is greater than 0.5

394

Sustain. Water Resour. Manag. (2016) 2:387–403

Table 3 Cross-validation results of GRNN for April

Forecasted variable: inflow to the reservoirs in April	Garsha	Tang Mashooreh	Seimareh	Karkheh
Best predictors				
Autumn projected series of Mediterranean Sea SST	✔	✔	✔	✔
Summer projected series of Persian Gulf SST	✔			
Winter projected series of Persian Gulf SST		✔		✔
Rainfall projected series in March	✔		✔	✔
Assessment criteria				
Nash–Sutcliff	0.774	0.701	0.667	0.874
RMSE	0.474	0.534	0.568	0.353
CORR	0.882	0.845	0.822	0.944

Table 4 Cross-validation results of GRNN for May

Forecasted variable: inflow to the reservoirs in May	Garsha	Tang Mashooreh	Seimareh	Karkheh
Best predictors				
Autumn projected series of Persian Gulf SST	✔	✔	✔	✔
Summer projected series of Persian Gulf SST	✔			
Rainfall projected series in March		✔		✔
Rainfall projected series in April	✔			
Streamflow in April	✔	✔	✔	✔
Assessment criteria				
Nash–Sutcliff	0.526	0.508	0.722	0.601
RMSE	0.688	0.697	0.526	0.632
CORR	0.832	0.784	0.875	0.864

Table 5 Cross-validation results of GRNN for June

Forecasted Variable: Inflow to the reservoirs in June	Garsha	Tang Mashooreh	Seimareh	Karkheh
Best predictors				
Streamflow in May	✔	✔	✔	✔
Assessment criteria				
Nash–Sutcliff	0.699	0.609	0.581	0.748
RMSE	0.549	0.626	0.647	0.502
CORR	0.849	0.783	0.770	0.872

the forecasting of the inflow to *Garsha*, *Seimareh*, and *Karkheh* reservoirs in April. The best predictors show that the streamflow in almost all the regions of *Karkheh* basin in April is affected by a combination of *Mediterranean Sea* SST and *Persian Gulf* SST. Comparing the best predictors of the reservoirs in April, it can be suggested that the predictors of *Garsha* and *Seimareh* reservoir are similar. Likewise, the predictors of *Tang Maghooreh* and *Karkheh* reservoirs are similar. The assessment criteria show that the accuracy of the *Karkheh* inflow forecast is more than other reservoirs. Figure 2 shows the point forecasts resulted from cross validation by the GRNN model for the best predictors, presented in Table 3, for April.

An assessment of the point estimation presented in Fig. 2 shows that the results of the GRNN model enjoy the appropriate accuracy. A detailed evaluation of this figure shows that the accuracy of the point estimations of

Garsha (a) and *Karkheh* (d) is better than *Tang Mashooreh* (b) and *Seimareh* (c). It can be seen from Fig. 2 that the maximum range of streamflow belongs to the inflow to *Garsha* reservoir which is between 248 and 1097 MCM. Although in the cross-validation analysis, 24 data have been used for calibrating the model for each run, and the point estimation shows that the model has been able to estimate well the data in a large range; only the error of the peak values is relatively high, because the number of them is few for training the model, but other values have a good accuracy.

Table 4 prominently shows that autumn projected series of *Persian Gulf* SST and streamflow in April are two of the best predictors for forecasting the inflow to all reservoirs. Like April, the summer projected series of *Persian Gulf* SST and rainfall projected series in previous month, i.e., April, are also effective predictors of inflow to *Garsha*
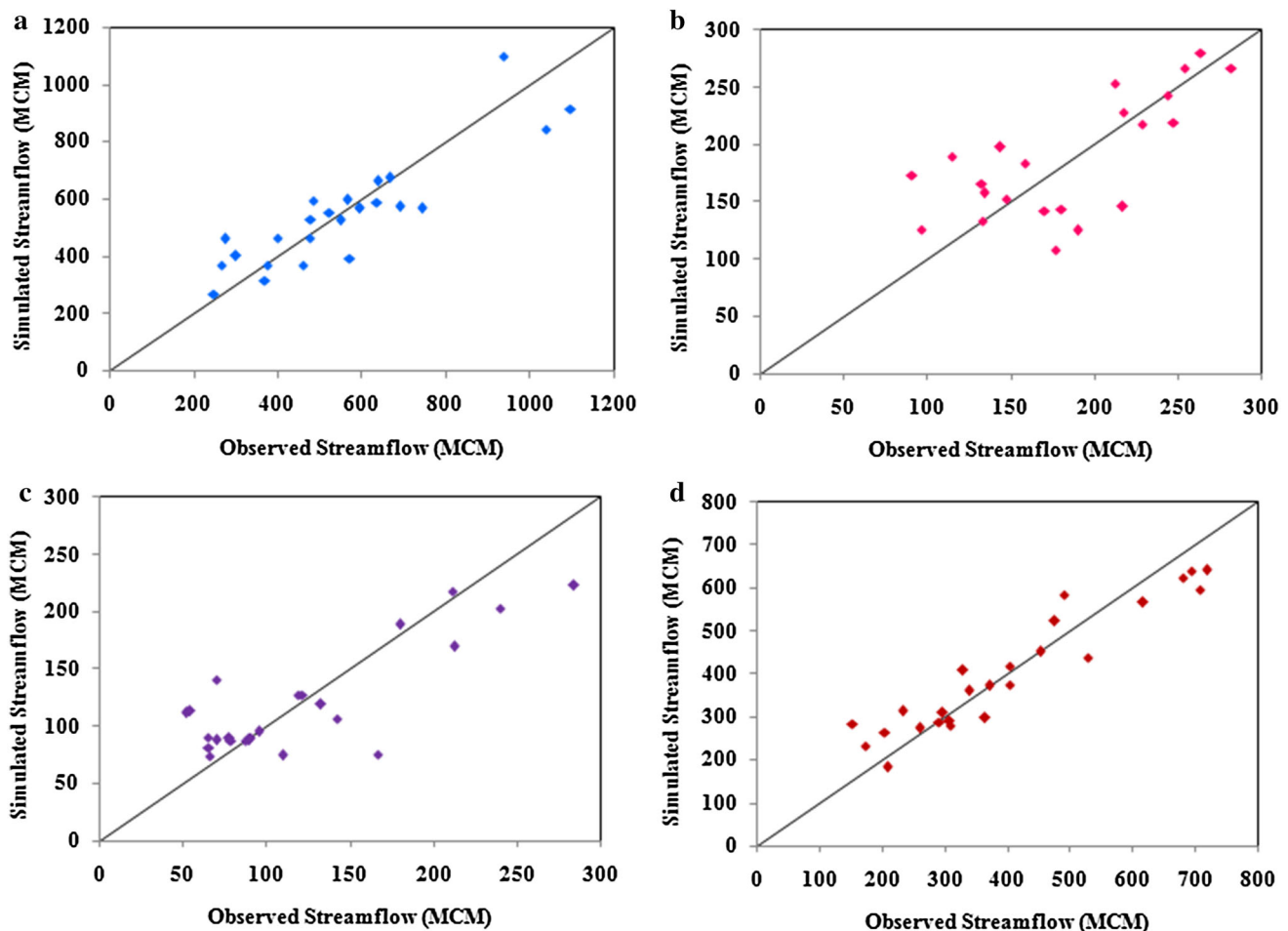
Fig. 2 Point forecasts of the GRNN model for *Garsha* (**a**), *Tang Mashooreh* (**b**), *Seimareh* (**c**), and *Karkheh* (**d**) reservoirs in April based on the best predictors

reservoir. Besides, rainfall projected series in March affects the inflow to *Tang Mashooreh* and *Karkheh* reservoirs. The comparison of the best predictors for all reservoirs in May reveals that the best predictors of *Tang Maghooreh* reservoir are the same as that of *Karkheh* reservoir. Moreover, the best predictors of *Garsha* and *Seimareh* reservoir are similar. The assessment criteria in this table show that the result of the *Seimareh* inflow forecasts is more accurate than the others and the accuracy of the results of *Garsha* and *Tang Mashooreh* is similar. Figure 3 illustrates the point forecasts resulted from cross validation by the GRNN model for the best predictors, presented in Table 4, for May.

It can be seen from Fig. 3 that the point estimations of *Garsha, Seimareh,* and *Karkheh* have a good accuracy; however, the reason why the assessment criteria present the low accuracy for the two reservoirs, *Garsha* and *Karkheh,* is the one and three estimations for high values for them, respectively. The lowest accuracy of the high-value estimations is due to their few numbers for training the model, because the number of extreme values is few. The

maximum range of inflow to the reservoirs in May belongs to *Garsha* (192–1072 MCM), and similar to April, the model has been able to estimate the inflow values (except the extreme value) appropriately, such that if the extreme value is omitted, the Nash–Sutcliff index will be 0.775.

Although a number of variables have been detected as appropriate predictors for forecasting the inflow to the reservoirs in June, the best results of the cross-validation analysis shown in Table 5 have been demonstrated that only the inflow to each reservoir in May is the best predictor for forecasting the inflow to each of ones in June. It is due to the fact that *Karkheh* Basin is located in a semiarid region, where significant precipitation does not occur from the late of May to the late of October. Therefore, as the climate variations affect the precipitation and consequently the streamflow, the inflow to the reservoirs in June is not affected by precipitation and the climate indices.

In Fig. 4, the point forecasts resulted from cross validation by the GRNN model for the best predictors, presented in Table 5, for June have been presented.
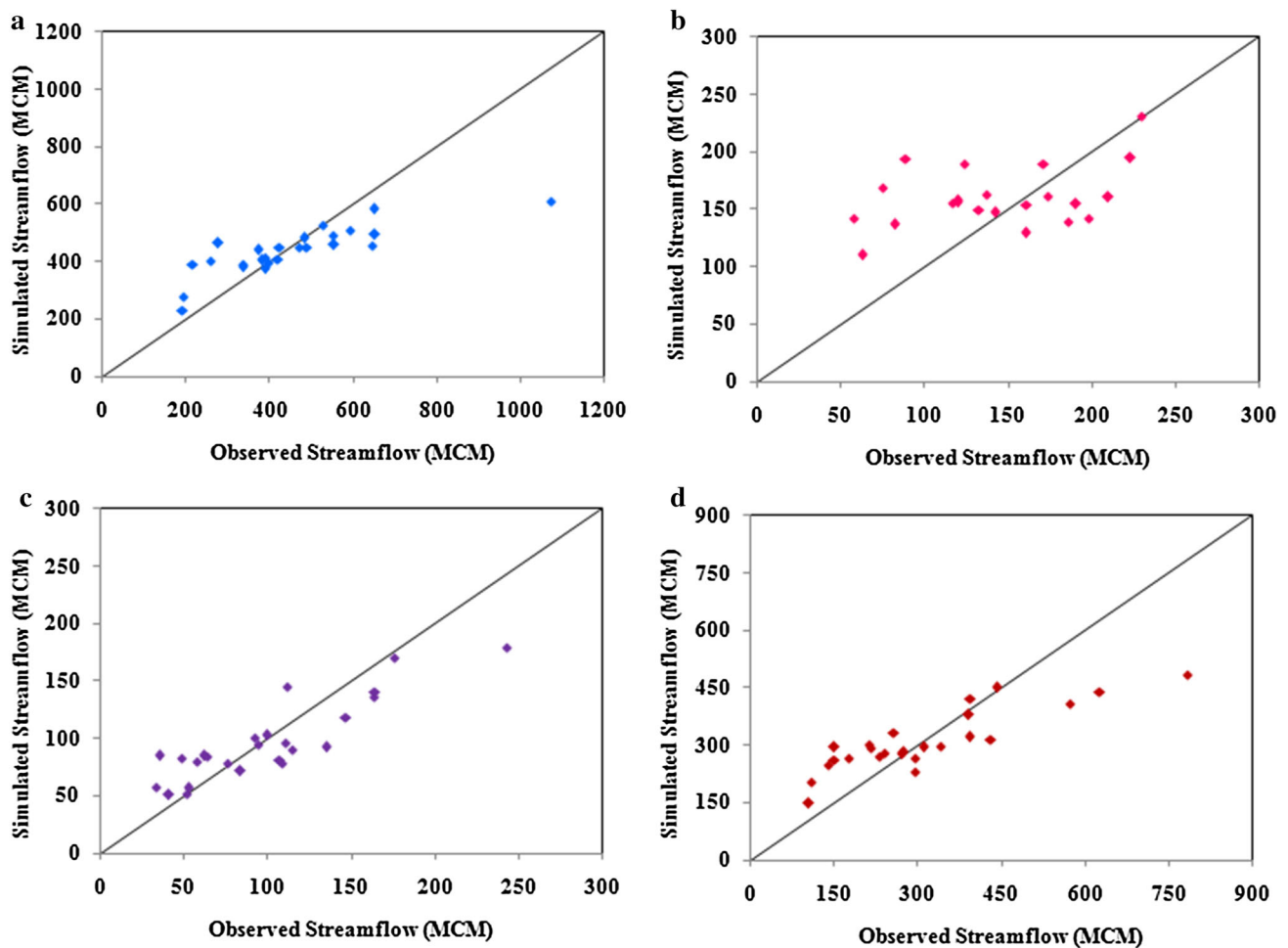
396

Sustain. Water Resour. Manag. (2016) 2:387–403

Fig. 3 Point forecasts of the GRNN model for *Garsha* (**a**), *Tang Mashooreh* (**b**), *Seimareh* (**c**), and *Karkheh* (**d**) reservoirs in May based on the best predictors

An assessment of the point estimations presented in Fig. 4 shows that while the results of *Garsha* and *Karkheh* are more accurate than the two others, the point estimation for all of them enjoys the enough accuracy.

Comparing the results presented in Tables 3, 4, and 5, it can be concluded that:

- The type of the best predictors in the north and west regions of *Karkheh* basin (*Garsha* and *Seimareh* subbasins) is similar in all the spring months. Likewise, the east and south regions of this basin (*Tang Mashooreh* and *Karkheh* subbasins) have similar pattern of predictors for streamflow forecasting.

- The inflow to *Garsha* reservoir in April and May is affected by summer SST of *Persian Gulf*. As the inflows to *Garsha* reservoir originate from the rivers in snowy regions and streamflow in April and May is resulted from snow melting, it can be suggested that the SST of *Persian Gulf* in the previous summer affects the

air temperature and, consequently, the amount of snow melting in the next spring in this region.

- Winter SST of *Persian Gulf* affects the streamflow in the east and south regions (*Tang Mashooreh* and *Karkheh* subbasins) of *Karkheh* basin in April. In the previous research (Nazemosadat 1998), it has been proved that the SST of *Persian Gulf* in winter has a significant correlation with the winter precipitation in the west and south provinces of Iran. The result of the present study is compatible with the previous study, because winter precipitation affects the streamflow in spring, especially April.

- Autumn SST of *Mediterranean Sea* has been detected as an effective variable for forecasting the inflow to all reservoirs in *Karkheh* basin in April. In the previous research (Meidani and Araghinejad 2014), it has been demonstrated that the autumn SST of *Mediterranean Sea* affects the winter precipitation in southwest of Iran, including *Karkheh* basin. The results of this study are consistent with the previous research, because on the
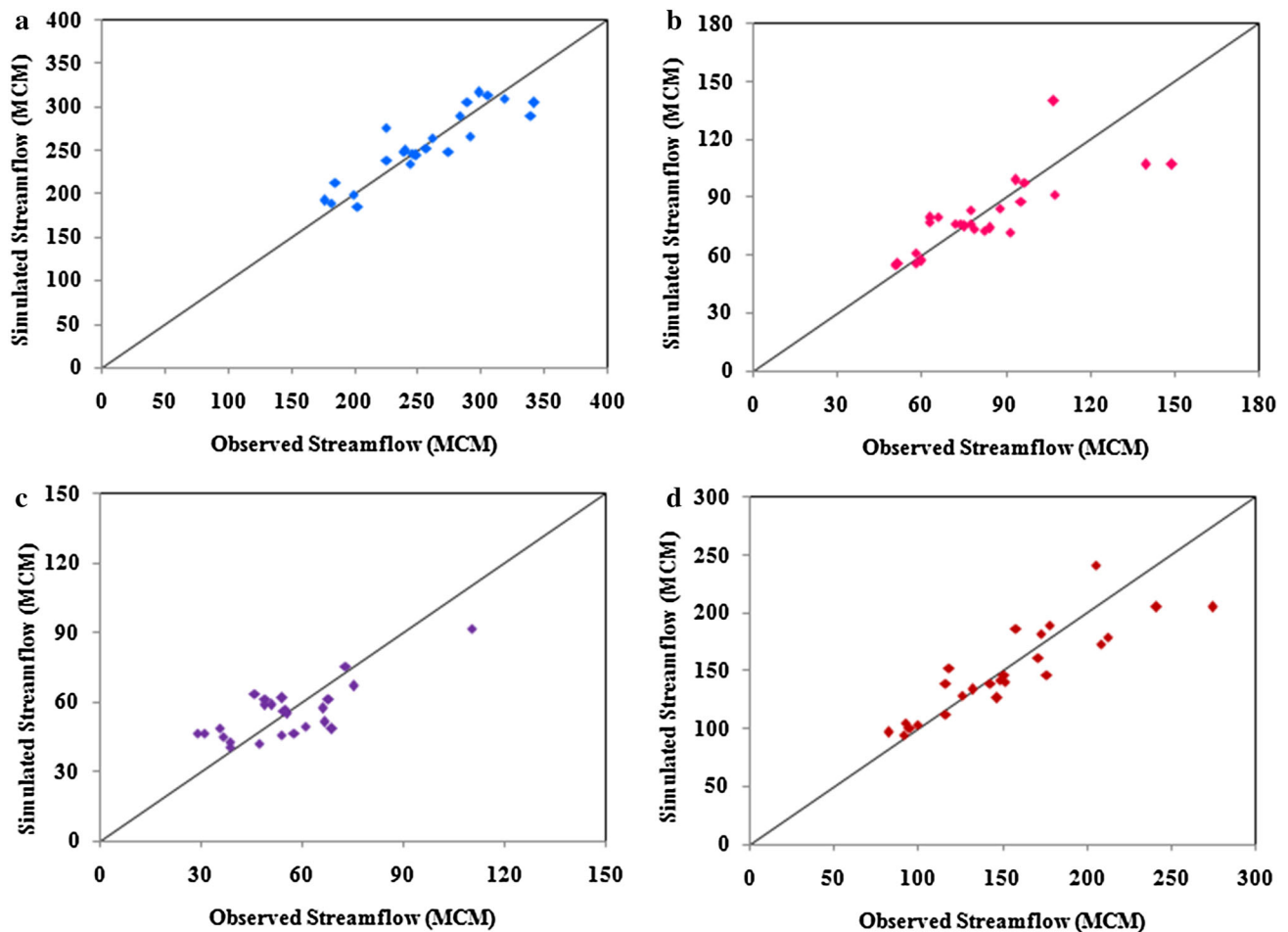
Sustain. Water Resour. Manag. (2016) 2:387–403

397

Fig. 4 Point forecasts of the GRNN model for *Garsha* (**a**), *Tang Mashooreh* (**b**), *Seimareh* (**c**), and *Karkheh* (**d**) reservoirs in June based on the best predictors

one hand, naturalized streamflow used in this study is affected directly by the precipitation, and on the other hand, winter precipitation affects the streamflow in spring.

- Autumn SST of *Persian Gulf* has been identified as one of the best predictors for forecasting the inflow to all reservoirs in *Karkheh* basin in May. In the previous study (Nazemosadat 2008), autumn SST of *Persian Gulf* has been applied for forecasting the precipitation in this season. The results of the present study suggest that like *Mediterranean Sea*, the SST of *Persian Gulf* in autumn affects the precipitation in winter and, as a result, affects the streamflow in spring.

- The inflows to all reservoirs except *Seimareh* in April are affected by a combination of *Mediterranean Sea* SST and *Persian Gulf* SST, while in May, the inflows to all reservoirs are affected by only SST of *Persian Gulf*. In contrary, the effect of local predictors, such as streamflow on the inflows to all reservoirs in June, is more than climate indices, such as SST of *Mediterranean Sea* and *Persian Gulf*.

To assess how the GRNN model has been fitted to the data in the best streamflow forecasts, shown their results in Tables 3, 4, and 5, the best values of the *Spread* parameter detected from the cross-validation analysis resulted in the best forecasts have been illustrated in Fig. 5. It is worth noting that the normal value for the *Spread* parameter is equal to one. The *Spread* values lower than one show that the function between input and output data has been closely approximated, while the *Spread* values larger than the typical value indicate the smoother function approximation.

It can be seen obviously from Fig. 5 that the GRNN model has been closely approximated the function between predictor and predicted data for all the four reservoirs for June, because the best values of the *Spread* parameter are lower than one for all of them. The little values of the *Spread* parameter indicate that the diversity of the observed data is small which can be due to the fact that only one predictor has been applied for forecasting the inflow to all reservoirs.

Another assessment of the Fig. 5 indicates that a considerably smooth function approximation has been done by
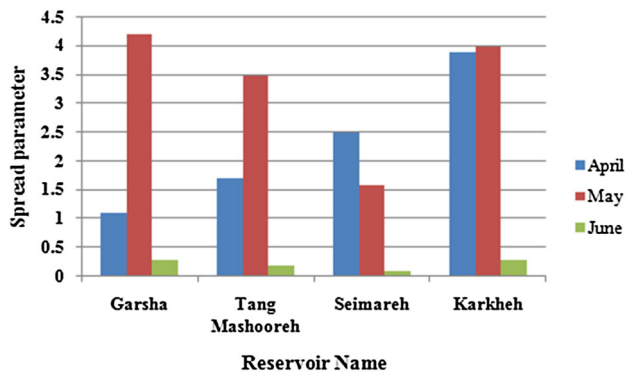
Fig. 5 Best values of the *Spread* parameter detected from the cross-validation analysis for the reservoirs in each month

the model for *Garsha* and *Tang Mashooreh,* in May, and for *Karkheh* in April and May, because of the large values of the *Spread* parameter (>3.5), while for *Garsha* and *Tang Mashooreh* in April, and for *Seimareh* in April and May, a smooth function approximation close to normal has been done by the model, due to the values between 1 and 2.5 for the *Spread* parameter. The larger *Spread* values identified as the best parameter values (from the range between 0.1 and 7 with the steps 0.1) by the model suggest that there are more complicated functions between predictors and

predicted data, which can be due to the variation of the predictors.

As autumn SSTs of *Mediterranean Sea* and *Persian Gulf* have been detected as effective predictors for forecasting the inflow to all reservoirs in April and May, respectively, to reveal the performance of them for streamflow forecasting, the GRNN model has been run for each reservoir three times for three states, including: only SST, best predictors without SST, and all the best predictors (with SST). Table 6 shows the assessment criteria resulted from the cross validation for three states for April. Table 7 presents similar results for May.

The assessment criteria presented in Table 6 show that applying only autumn SST of *Mediterranean Sea* as predictor leads to the best result for forecasting the inflow to *Karkheh* reservoir in April in comparison with other reservoirs. The comparison of the results obtained from using single SST (case 1) and best predictors without SST (case 2) reveals that the results of case 2 for *Garsha* and *Seimareh* reservoirs are better than case 1. Instead, the results of case 1 for *Tang Mashooreh* and *Karkheh* reservoir are better than case 2. However, the assessment criteria show that applying autumn SST along with other best predictors (case 3) produces the best forecasts in comparison with two other cases for all reservoirs. The forecasts in

Table 6 Cross-validation results of streamflow forecasting in the three states of predictors for April

Predictor	Assessment criteria	Garsha	Tang Mashooreh	Seimareh	Karkheh
Autumn SST of Mediterranean Sea	Nash–Sutcliff	0.357	0.436	0.374	0.733
	RMSE	0.799	0.733	0.779	0.514
	Correlation coefficient	0.626	0.677	0.625	0.878
Best predictors without Mediterranean SST	Nash–Sutcliff	0.661	0.419	0.608	0.568
	RMSE	0.580	0.744	0.617	0.655
	Correlation coefficient	0.818	0.698	0.813	0.767
Best predictors with Mediterranean SST	Nash–Sutcliff	0.774	0.701	0.667	0.874
	RMSE	0.474	0.534	0.568	0.353
	Correlation coefficient	0.882	0.845	0.822	0.944

Table 7 Cross-validation results of streamflow forecasting in the three states of predictors for May

Predictor	Assessment criteria	Garsha	Tang Mashooreh	Seimareh	Karkheh
Autumn SST of Persian Gulf	Nash–Sutcliff	0.405	0.427	0.525	0.468
	RMSE	0.771	0.752	0.688	0.729
	Correlation coefficient	0.641	0.656	0.728	0.695
Best predictors without Persian Gulf SST	Nash–Sutcliff	0.519	0.441	0.358	0.372
	RMSE	0.693	0.742	0.800	0.792
	Correlation coefficient	0.746	0.683	0.615	0.709
Best predictors with Persian Gulf SST	Nash–Sutcliff	0.526	0.508	0.722	0.601
	RMSE	0.688	0.697	0.526	0.632
	Correlation coefficient	0.832	0.784	0.875	0.864

Sustain. Water Resour. Manag. (2016) 2:387–403

399
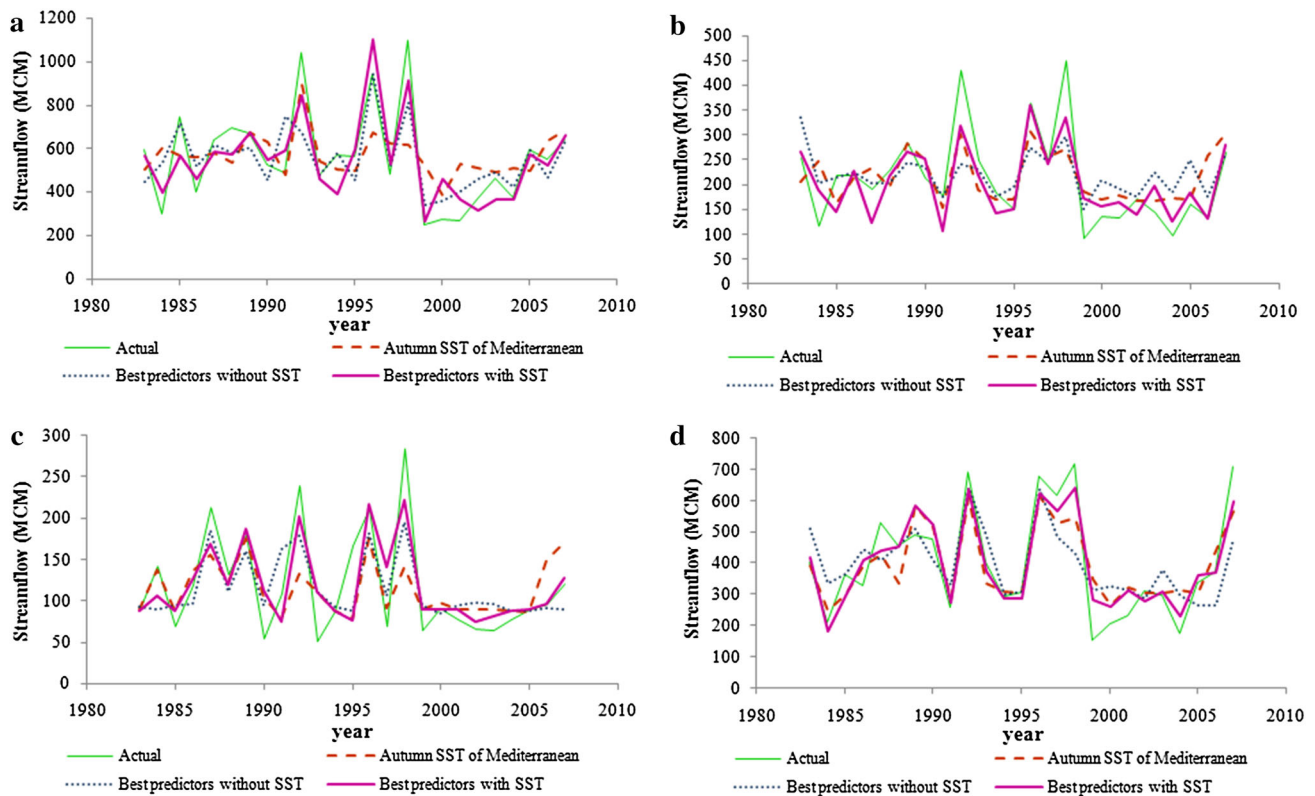
Fig. 6 Estimated inflow to *Garsha* (**a**), *Tang Mashooreh* (**b**), *Seimareh* (**c**), and *Karkheh* (**d**) reservoirs in April according to the three states of predictors

this case lead to maximum Nash–Sutcliff and minimum RMSE. In addition, in this case, there is maximum CORR between observed and estimated streamflows. It is worth noting that applying each of the climate variables of the best predictors singly results in less accuracy than applying all the best predictors. For example, the results of case 2 for *Tang Mashooreh* have been obtained from the use of only winter SST of *Persian Gulf* as a single predictor. In Fig. 6, the estimated inflow to *Garsha* (a), *Tang Mashooreh* (b), *Seimareh* (c), and *Karkheh* (d) reservoirs for the three cases of predictors in April has been illustrated and compared with the actual inflow.

The assessment criteria in Table 7 indicate that the use of only autumn SST of *Persian Gulf* as predictor for streamflow forecasting (case 1) in May results in better results for *Seimareh* and *Karkheh* in comparison with the use of other best predictors (case 2). In contrary, for *Garsha* and *Tang Mashooreh,* the results of case 2 are better than case 1. However, the assessment criteria in Table 7 demonstrate that, like April, applying autumn SST of *Persian Gulf* along with other best predictors (case 3) results in the best forecasts in comparison with two other cases for all reservoirs. Figure 7 shows the estimated inflow to *Garsha* (a), *Tang Mashooreh* (b), *Seimareh* (c), and *Karkheh* (d) reservoirs in May for the three cases of

predictors, while they have been compared with the actual inflow.

Summary and conclusion

In this study, the combined effect of seasonal Sea Surface Temperature (SST) of *Persian Gulf* and *Mediterranean Sea* on operational streamflow forecasting in *Karkheh* basin in spring months was investigated regionally. For this purpose, forecasting of the monthly inflow to four reservoirs in this basin, each of which collects the outflow of a subbasin, was considered. Besides, in this paper with the goal of reducing the forecasting errors, rather than doing two process, including forecasting of precipitation and rainfall-runoff modeling to achieve the streamflow forecasting, the direct effect of *Mediterranean Sea* and *Persian Gulf* SST on streamflow forecasting has been studied.

The research was done in three steps. In the first step, the singular value decomposition (SVD) method was used to determine the effective nodes of *Mediterranean Sea* and *Persian Gulf* on the climate of the subbasins of *Karkheh* basin and to produce the most correlated time series of SST with the streamflow of each subbbasin. Besides, this method was applied to create rainfall time series of rain
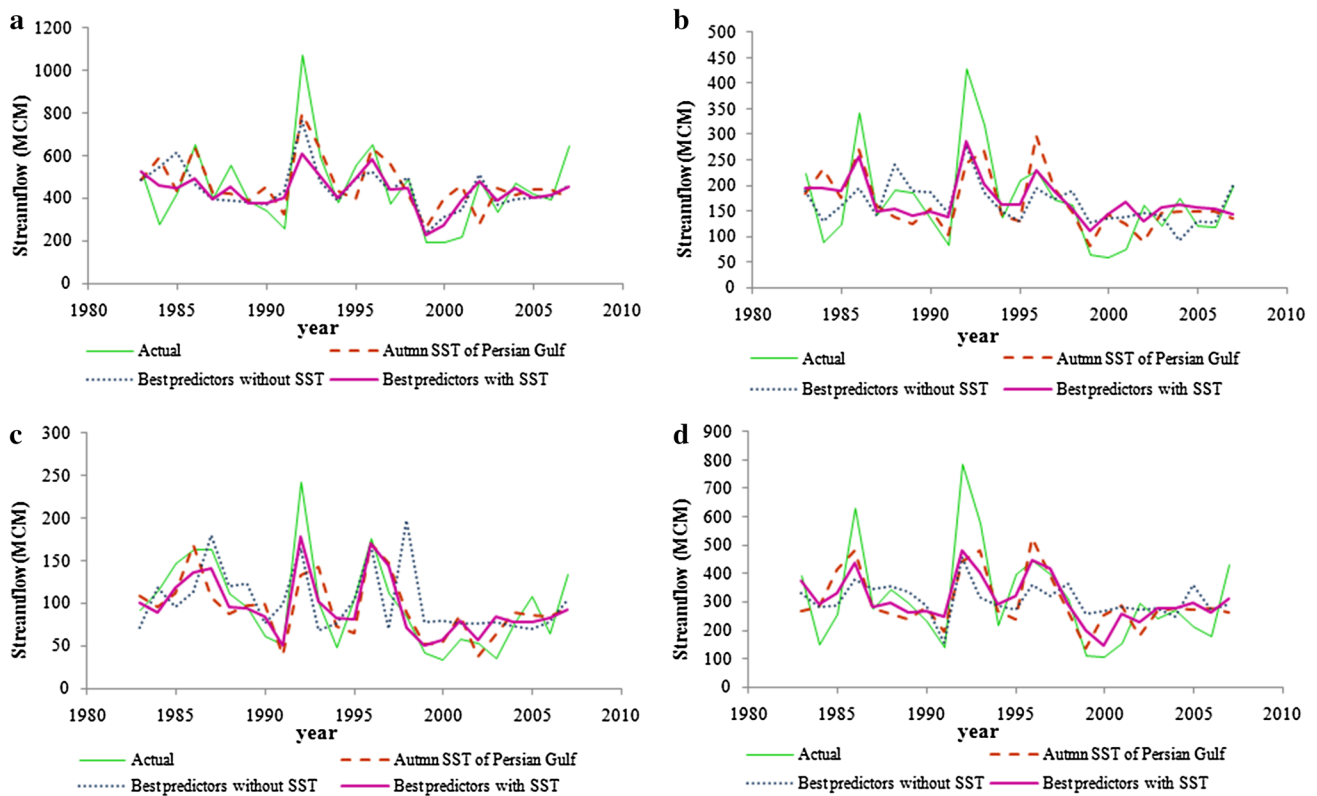
Fig. 7 Estimated inflow to *Garsha* (**a**), *Tang Mashooreh* (**b**), *Seimareh* (**c**), and *Karkheh* (**d**) reservoirs in May according to the three states of predictors

stations, such that they had higher correlation with the inflow to each reservoir than the average of the rainfall of the stations.

In the second step, the appropriate predictors for forecasting the inflow to each reservoir were determined from the seasonal projected series of SST and hydrological and meteorological data based on two evaluation criteria, including: correlation coefficient (R^2) and MMI index which is based on Mutual Information (MI) and entropy rules.

In the last step, the best predictors were determined for each reservoir from several combinations of the appropriate predictors based on the cross-validation analysis for the results of GRNN model.

The results indicated that all the nodes of *Persian Gulf* and *Mediterranean Sea* affect the study region, because the SCF of first mode was above 95 % in all the cases.

In addition, autumn SSTs of *Mediterranean Sea* and *Persian Gulf* were detected as effective predictors for forecasting the inflow to all reservoirs in *Karkheh* basin in April and May, respectively. The results also revealed that winter SST of *Persian Gulf* affected the streamflow in the east and south regions (*Tang Mashooreh* and *Karkheh* subbasins) of *Karkheh* basin in April, while the inflow to *Garsha* reservoir in April and May was affected by summer

SST of *Persian Gulf*. All the results of this research were compatible with the previous research (Nazemosadat 1998; Nazemosadat 2008; Meidani and Araghinejad 2014). In addition, the obtained results showed that the best predictor for forecasting the inflow to all reservoirs in June was the inflow to them in May.

The assessment of the results of the GRNN model parameter (*Spread* parameter) indicated that for June, model approximated closely the functions between predictor and predicted variables, while for two other months, smoother function approximation has been done by the model. The evaluation of the results of *Spread* parameter with respect to the number of predictors for each reservoir and month showed that when the number of predictors increased, the optimum value of the *Spread* parameter was also increased, and as a result, smoother functions were approximated by the model.

Considering the results of this study, it can be concluded that:

- The SSTs of *Persian Gulf* and *Mediterranean Sea* in autumn are effective predictors for spring streamflow forecasting in all the subbasins in *Karkheh* basin, because they affect winter precipitation throughout the basin and spring streamflow is affected by winter precipitation.

- Summer SST of *Persian Gulf* has been detected as an effective predictor for streamflow forecasting in April and May in snowy regions. It may be due to the effect of Summer SST on air temperature in the next spring, and as a result, it affects the amount of snow melting.
- It has been detected that winter SST of *Persian Gulf* is an effective predictor for streamflow forecasting in April in the east and south regions of *Karkheh* basin, because it affects winter precipitation in this region.
- The combination of the *Mediterranean Sea* SST and *Persian Gulf* SST affects the streamflow in almost all the regions of the basin in April, while the streamflow in May is affected by *Persian Gulf* SST.
- Although several variables have high correlation with the streamflow in June, the streamflow in May is the most effective predictor for forecasting the streamflow in June throughout the basin. It is due to the fact that *Karkheh* basin is located in a semiarid region, where a significant precipitation does not occur from the late of May to the late of Octobr. Therefore, as the climate variations affect the precipitation and, consequently, the streamflow, the inflow to the reservoirs in June is not affected by the precipitation and the climate indices.
- The north and west regions of *Karkheh* basin (*Garsha* and *Seimareh* subbasins) have similar pattern of the best predictors for operational streamflow forecasting. Likewise, the best predictors of the east and south regions of this basin (*Tang Mashooreh* and *Karkheh* subbasins) are similar in all the spring months.

All in all, as a final conclusion of the obtained results of this study, it can be said that:

1. The regional streamflows in *Karkheh* basin in April and May are affected by the SST of *Mediterranean Sea* and *Persian Gulf* and the appropriate accuracy of the operational forecasting results indicate that the climate variables are applicable and effective predictors for operational streamflow forecasting in regional scale if the naturalized streamflow, affected directly by precipitation, is applied.
2. The good results of forecasting the naturalized streamflow using climate indices indicate that this approach can be used to streamflow forecasting rather than doing two process, including the forecasting of precipitation and rainfall-runoff modeling.
3. In a large basin with several climate, the effect of climate variations on the meteorological and hydrological responses of the basin can be different; such that in the mountainous region of the *Karkheh* basin, the effect of summer SST of *Persian Gulf* has been detected on the streamflow in April and May, which may be due to its effect on air temperature in the next

spring and, consequently, its effect on the amount of snow melting, while it has not affected the streamflows of other regions of the basin.

4. In *Karkheh* basin, the pattern of streamflow predictors for spring months in the north and west regions which are mountainous area with cold winters and mild summers is similar, while the east and south regions of the basin which are semiarid area with mild winters and long and warm summers also have similar pattern of predictors for spring months.
5. With respect to the results of the previous studies (Nazemosadat 1998; Nazemosadat 2008; Meidani and Araghinejad 2014) proved that winter precipitation in the west of Iran is affected by autumn SST of *Mediterranean Sea* and *Persian Gulf* and the obtained results in this study, it can be concluded that the naturalized streamflow in the *Karkheh* basin in spring is directly affected by the precipitation in winter.
6. As the Sudan current from the *Persian Gulf* and the moist air masses originated from *Mediterranean Sea* affect the precipitation in south and west of Iran in winter on the one hand, and on the other hand, in the previous studies and in the current study, it has been proved that the SST of *Mediterranean Sea* and *Persian Gulf* in autumn affects the winter precipitation and, consequently, spring streamflows, it can be suggest that probably, there is a relation between the SST of the *Mediterranean Sea* and *Persian Gulf* in autumn and the formation of rainy air masses in winter which affects the winter rainfall in Iran. It is recommended that the hypothesis be survey in another research.
7. The GRNN model which enjoys a radial basis function is able to approximate the complicated functions between several predictors and predicted variables and produces the forecasting results with the appropriate accuracy in monthly scale.

Finally, it is recommended that a research be also done using the wavelet transform analysis for preprocessing the inputs of forecasting model and the accuracy of the achieved results be compared with the current research. Moreover, it is suggested that in another study, the relation between the climate indices and snow cover area, resulted from MODIS/AVHRR images, be investigated.

References

Anctil F, Rat A (2005) Evaluation of neural network streamflow forecasting on 47 watersheds. J Hydrol Eng 10(1):85–88

Araghinejad S (2014) Data-driven modeling: using MATLAB® in water resources and environmental engineering. Water science and technology library, vol 67. Springer, Netherlands

Araghinejad S, Burn DH, Karamouz M (2006) Long-lead probabilistic forecasting of streamflow using ocean-atmospheric and hydrological predictors. J Water Resour Res 42(3):W03431. doi:10.1029/2004WR003853

Azimi M, Golpaygani F, Tajrishy M, Abrishamchi A (2011) Seasonal prediction of Karoon streamflow using large-scale indices. World Environ Water Resour Congress 1184–1193

Bretherton CS, Smith C, Wallace JM (1992) An intercomparison of methods for finding coupled patterns in climate data. J Climate 5:541–560

Cigizoglu HK (2005) Generalized regression neural network in monthly flow forecasting. J Civil Eng Environ Syst 22(2):71–81

Cigizoglu HK, Alp M (2004) Rainfall-runoff modelling using three neural network methods. J Artificial Intell Soft Comput 3070:166–171

Clark CO, Cole JE, Webster PJ (2000) Indian Ocean SST and Indian summer rainfall: predictive relationships and their decadal variability. J Climate 13:2503–2519

Dezfuli AK, Karamouz M, Araghinejad S (2010) On the relationship of regional meteorological drought with SOI and NAO over southwest Iran. Theoret Appl Climatol 100:57–66

Gamiz-Fortis SR, Esteban-Parra MJ, Trigo RM, Castro-Diez Y (2010) Potential predictability of an Iberian river flow based on its relationship with previous winter global SST. J Hydrol 385:143–149

Gray RM (2013) Entropy and information theory. Springer-Verlag, NewYork

Hamlet A, Lettenmaier D (1999) Columbia river streamflow forecasting based on ENSO and PDO climate signals. J Water Resour Plann Manage 125(6):333–341

Hosseini-Moghari SM, Araghinejad S (2015) Monthly an seasonal drought forecasting using statistical neural networks. Environ Earth Sci 74(1):397–412

Karla A, Ahmad S (2009) Using oceanic-atmospheric oscillations for long lead time streamflow forecasting. J Water Resour Res 45:W03413. doi:10.1029/2008WR006855

Kassomenos PA, McGregor GR (2006) The inter annual variability and trend of precipitable water over Southern Greece. J Hydrometeorol 7:271–284

Kendrew WG (1922) The climates of the continents. Oxford University Press

Khalili A (1992) Fundamental study of Iranian water resources, climatological understanding of Iran, Parts 1 and 2. Jamab consultant reports, the Iranian Ministry of Energy (**in Persian**)

Kişi Ö (2008) River flow forecasting and estimation using different artificial neural network techniques. Hydrol Res 39(1):27–40

Kutiel H, Hirsch-Eshkol TR, Türkeş M (2001) Sea level pressure patterns associated with dry or wet monthly rainfall conditions in Turkey. Theor Appl Climatol 69(1–2):39–67

Lima CHR, Lall U (2010) Climate informed monthly streamflow forecasts for the Brazilian hydropower network using a periodic ridge regression model. J Hydrol 380(3):438–449

Lorenzo-lacruz J, Vicente-Serrano SM, Lopez-Moreno JI, Gonzalez-Hidalgo JC, Moran-Tejeda E (2011) The response of Iberian rivers to the North Atlantic oscillation. Hydrol Earth Syst Sci 15:2581–2597

Meidani E, Araghinejad S (2014) Long-lead streamflow forecasting in the southwest of Iran by sea surface temperature of the Mediterranean Sea. J Hydrol Eng 19(8):05014005

Meng X, Maosheng Y, Ning L, Li D, Xue X (2015) A threshold artificial neural network model for improving runoff prediction in a karst watershed. Environ Earth Sci. doi:10.1007/s12665-015-4562-9

Nash JE, Sutcliffe JV (1970) River flow forecasting through conceptual models part I—a discussion of principles. J Hydrology 10(3):282–290

Nazemosadat MJ (1998) The Persian Gulf sea surface temperature as a drought diagnostic for southern parts of Iran. Drought News Netw 10:12–14

Nazemosadat MJ (2008) Improving neural network models for forecasting seasonal precipitation in southwestern Iran: the evaluation of oceanic-atmospheric indices. Adv Geosci 16:133–145

Nicholls N (1989) Sea surface temperature and Australian winter rainfall. J Climate 2:965–973

Oubeidillah AA, Tootle GA, Moser C, Piechota T, Lamb K (2011) Upper Colorado River and Great Basin streamflow and snowpack forecasting using Pacific oceanic–atmospheric variability. J Hydrol 410:169–177

Oubeidillah AA, Tootle G, Anderson SR (2012) Atlantic Ocean sea-surface temperatures and regional streamflow variability in the Adour-Garonne basin, France. Hydrol Sci J 57(3):496–506

Perrone TJ (1979) Winter shamal in the Persian Gulf. Naval Env Prediction Res Facility, Technical Report, pp 79–96

Rodriguez-Fonseca B, de Castro M (2002) On the connection between winter anomalous precipitation in the Iberian Peninsula and North West Africa and the summer subtropical Atlantic sea surface temperature. Geophys Res Lett 29(18):1863. doi:10.1029/2001GL014421

Rowell DP (2003) The impact of Mediterranean SSTs on the Sahelian rainfall seasonal. J Clim 16(5):849–862

Sagarika S, Kalra A, Ahmad S (2015) Pacific Ocean SST and Z_{500} climate variability and western US seasonal streamflow. Int J Climatol. doi:10.1002/joc.4442

Sattari MT, Apaydin H, Ozturk F (2012) Flow estimations for the Sohu Stream using artificial neural networks. Environ Earth Sci 66(7):2031–2045

Sharma A (2000) Seasonal to interannual rainfall probabilistic forecasts for improved water supply management: Part 1—a strategy for system predictor identification. J Hydrol 239:232–239

Skiliris N, Sofianos S, Gkanasos A, Mantiziafo A, Vervatis V, Axaopoulos P, Lascaratos A (2011) Decadal scale variability of sea surface temperature in the Mediterranean Sea in relation to atmospheric vriability. Ocean Dyn. doi:10.1007/s10236-011-0493-5

Soukup TL, Aziz OA, Tootle GA, Piechota TC, Wulff SS (2009) Long lead-time streamflow forecasting of the North Platte River incorporating ocean-atmospheric climate variability. J Hydrol 368:131–142

Tabari H, Abghari H, Hosseinzadeh Talaee P (2013) Impact of the North Atlantic oscillation on streamflow in western Iran. Hydrol Process. doi:10.1002/hyp.9960

Thoppil PG, Hogan PJ (2010) Persian Gulf response to a wintertime shamal wind event. Deep-Sea Res 1(57):946–955

Tootle GA, Piechota TC (2006) Relationships between Pacific and Atlantic Ocean sea surface temperatures and US streamflow variability. Water Resour Res 42:W07411. doi:10.1029/2005WR004184

Tootle GA, Singh A, Piechota T, Farnham I (2007) Long lead-time forecasting of US streamflow using partial least squares regression. J Hydrol Eng 12(5):442–451

Tootle GA, Piechota TC, Gutierrez F (2008) The relationships between Pacific and Atlantic Ocean Sea surface temperatures and Colombian streamflow variability. J Hydrol 349:268–276

Uvo CB, Repelli CA, Zebiak SE, Kushnir Y (1998) The relationship between tropical Pacific and Atlantic SST and northeast Brazil monthly precipitation. J Climate 11:551–562

Wallace JM, Smith C, Bretherton CS (1992) Singular value decomposition of wintertime sea surface temperature and 500-mb height anomalies. J Climate 5:561–576

Wang H, Ting M (2000) Covariabilities of winter US precipitation and pacific sea surface temperatures. J Climate 13:3711–3719

Wang WC, Chau KW, Cheng CT, Qui L (2009) A comparison of performance of several artificial intelligence methods for forecasting monthly discharge time series. J Hydrology 374:294–306

Wu CL, Chau KW, Fan C (2010) Prediction of rainfall time series using modular artificial neural networks coupled with data preprocessing techniques. J Hydrol 389:146–167